Published in Applied Physics Letters 89, issue 061119, 1-3, 2006
which should be used for any reference to this work

23 GHz operation of a room temperature photovoltaic quantum cascade detector at 5.35 μm

Daniel Hofstetter, Marcel Graf[a], Thierry Aellen, and Jérôme Faist
University of Neuchâtel, Institute of Physics, 1 A.-L. Breguet, CH-2000 Neuchâtel, Switzerland
Lubos Hvozdara and Stéphane Blaser
Alpes Lasers SA, Passage Maximilien-de-Meuron 1-3, CH-2000 Neuchâtel, Switzerland

We present a room temperature operated 5.35 μm quantum cascade detector which was tested at high frequencies using an optical heterodyne experiment. Two slightly detuned continuous wave distributed feedback single mode quantum cascade lasers were used to generate a beating signal. The maximum frequency at which the resulting microwave signal could be detected was 23 GHz. The cutoff behavior of our device was modeled with a simple *RLC* circuit and showed excellent agreement with the experimental data.

Recently, there has been an increasing interest for photovoltaic quantum cascade detectors (QCDs).[1–3] Their operation principle is based on intersubband transitions in quantum wells embedded in an asymmetric, saw-tooth-like conduction band structure, which allows transport of the excited electrons in one direction only. Apart from the drawback of a lacking photoconductive gain,[4] such devices offer several advantages over photoconductive quantum well infrared photodetectors (QWIPs). Since no bias voltage must be applied, no dark current flows; therefore, QCDs do not suffer from dark current noise. This has been nicely illustrated by the fabrication of a GaAs/AlGaAs-based 87 μm far-infrared QCD by Graf *et al.*[5] In fact, Johnson noise rather than dark current noise is the dominant noise mechanism in these devices. Second, the optical transition between two bound states in a single active well leads to reduced interface scattering and therefore a narrow linewidth of <10 meV. Since the background radiation seen by such devices is minimized due to this small linewidth, the background limited operating regime can potentially be extended to higher temperatures than in a QWIP. Third, the absence of a dark current allows, in principle, the fabrication of arrays with small power dissipation and the use of long integration times to increase sensitivity without saturating the charge-coupled device readout circuit. Up to now, it was not clear whether QCDs would be equally suitable for high frequency experiments as QWIPs.[6] On the other hand, it is evident that fast midinfrared detectors have in general interesting applications in astronomical heterodyne interferometry both in space and on Earth,[7] but also in the characterization of ultrafast laser pulses.[8] In the work described below, we want to stress the point that such QCDs can indeed be very fast. In order to conveniently characterize our devices, we used two slightly detuned continuous wave (CW) operated distributed feedback (DFB) quantum cascade lasers which generated, via heterodyning, an optical signal modulated at microwave frequencies of up to 23 GHz.[9] At this frequency, the detector signal decreased by a factor of 50 as compared to the one observed at 3 GHz. However, a simple numerical model taking into account the parasitic capacitance due to the size of the QCD (100×100 μm^2) and the inductance of the bonding wire with a length of 2.5 mm confirmed that device geometry and electrical wiring rather than the physics of the QCD were the limiting factors for high frequency operation. It is expected that the intrinsic cutoff frequency of such a device can reach similarly high values as in a QWIP, namely, several tens of gigahertz.[10,11]

Fabrication of our structures relied on molecular beam epitaxy of a 30 period chirped InGaAs/InAlAs superlattice (SL) active region grown lattice matched on a semi-insulating InP substrate. Below and above the SL, two Si-doped (1.6×10^{18} cm^{-3}) InGaAs contact layers were deposited. The thicknesses were 200 nm for the top layer and 600 nm for the bottom contact. The layer thicknesses of the InAlAs barriers (bold) and the InGaAs wells (roman) between two subsequent active wells were adjusted in order to provide a phonon ladder; i.e., six bound states with an energy separation of a longitudinal optical phonon (32 meV) between each state (59/**60**/17/**44**/20/**39**/23/**37**/27/**35**/32/**31**/49/**28**/47/**26** Å, underlining means doping, Si, 4×10^{17} cm^{-3}). This arrangement is important for an ultrafast vertical transport of the excited electrons into the ground state of the following period.[12] The upper state of the transition is a duplet state which leads to a theoretical escape probability of 50% into the phonon ladder region. A schematic conduction band diagram with the most important wave functions and the layer thicknesses in the active region is shown in Fig. 1. Processing relied on chemical wet etching of square mesa structures with a side length of 100, 200, or 300 μm. Electrical contacts were formed by a standard lift-off deposition of Ti/Au/Ge/Ag/Au layers (1.5/12/27/150/350 nm). The samples were cleaved and polished at an angle of 45° in order to offer a coupling geometry which is compatible with the polarization selection rule for intersubband transitions.[13] For the measurement of the spectral and dc electric properties of the QCD, the device was then mounted on a copper heat sink and wire bonded to a Au-plated ceramic platelet. *I-V* characteristics of the smallest mesas revealed a resistance in excess of 20 MΩ at 10 K

[a]Electronic mail: daniel.hofstetter@unine.ch

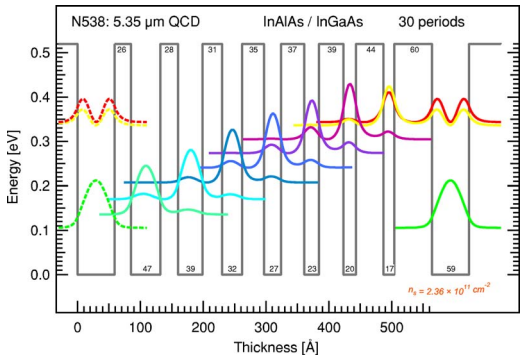

FIG. 1. (Color online) Relevant wave functions and conduction band diagram of one period of a QCD for 1850 cm^{-1} (5.35 μm). The phonon ladder for vertical electron transport is very well visible in this schematic drawing.

and on the order of 1 kΩ at 300 K. Small kinks at specific voltages in the *I-V* curve confirmed the existence of particular alignment situations in which, for instance, the first phonon ladder state was aligned with the ground state of the next period. Since the detector works at 0 V bias, these kinks are of no further relevance for the operation of the device. The spectral measurements as a function of temperature typically revealed spectra as the ones shown in Fig. 2. They were measured in the sample compartment of a Fourier transform infrared (FTIR) spectrometer under illumination with the internal glow-bar infrared light source. The detector signal was amplified by a Stanford Research SR570 low-noise current preamplifier and fed into the external port of the FTIR. The central wavelength of the QCD slightly shifted with increasing temperature from 1880 cm^{-1} at 10 K to 1830 cm^{-1} at 300 K while the linewidth remained constant at 10 meV. For the heterodyne experiments, the detector was glued directly on a high frequency connector, connected to its central conductor with a short bond wire, and tested at room temperature only.

Double-pass intersubband absorption of the detector at room temperature peaks at 7.2% absorption for 1830 cm^{-1}, agrees nicely with its spectral responsivity curve at 300 K, and corresponds to the expected absorption strength of 7.5% computed via Fermi's golden rule. The (irrelevant) absorption length, L_{dev}, in this case is twice the active region thick-

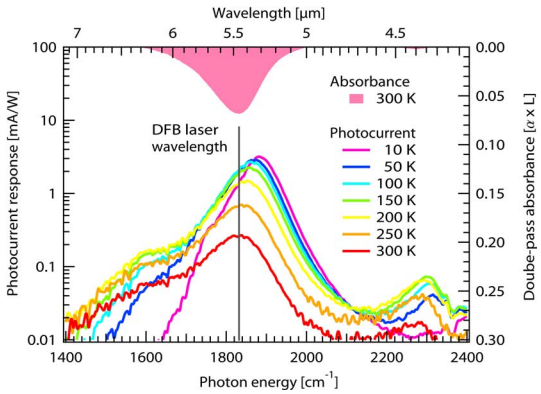

FIG. 2. (Color online) Standing on the bottom *x* axis: spectral response curves of the QCD at 5.35 μm as a function of temperature (from top to bottom: 10, 50, 100, 150, 200, 250, and 300 K). Hanging from the top *x* axis, the double-pass absorption spectrum at room temperature is shown. The spectral position of one of the DFB lasers is also shown at 1832 cm^{-1} (5.46 μm).

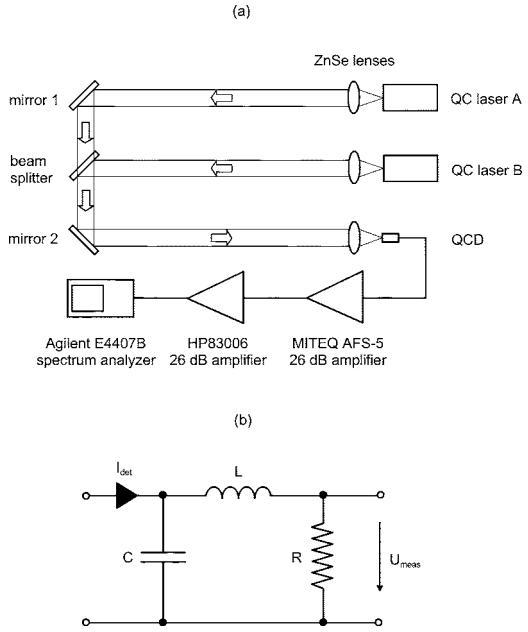

FIG. 3. (Color online) (a) Schematic drawing of the optical heterodyne setup. The two QCL beams are overlaid from behind the beam splitter and until they reach the QCD. (b) Electric *RLC* circuit which was used for fitting the measured cutoff behavior.

ness times a geometrical factor (L_{dev}=4 μm). For the absorption measurement, however, a multipass configuration with five double passes was used. Such measurements are usually done on large area samples with a total size of 3 ×3 mm^2. The maximal responsivity was obtained by dividing the measured photovoltage by the device resistance and the incoming light power. A rough estimation shows that our device falls roughly a factor of 1.7 short of the maximal possible value (3.2 mA/W instead of theoretically possible 5.6 mA/W based on the above absorption). This can be explained by a 30% (instead of 50%) escape probability out of the main well.

In order to achieve a high frequency modulation with constant amplitude, optical heterodyning was employed. In this experiment, which is schematically shown in Fig. 3(a), two collimated CW single mode midinfrared laser beams, which were emitted by two identical DFB QCLs, were collinearly overlaid. After a common optical path length of roughly 1 m, the two beams were focalized onto the QCD. Laser A was operated at a temperature of −18 °C and a dc current between 450 and 500 mA (25 mW output power), whereas laser B was held at −33 °C and operated at 320 mA (8 mW output power). These parameters resulted in an emission wavelength of 1832 cm^{-1} (5.46 μm) for both lasers; the spectral position of one device is shown in Fig. 2. The current tuning of laser A was sufficiently large to generate a beating frequency in excess of 20 GHz (0.7 cm^{-1}) between the two wavelengths. Using low-loss microwave cables, the detector was first connected to a low-noise high frequency voltage amplifier (MITEQ AFS-5, 26 dB) with a cutoff frequency of 21 GHz. In series with this first voltage amplifier, we connected a second one (HP83006, 26 dB) whose cutoff frequency was at 26.5 GHz. From the output of this second amplifier, another low-loss cable connected to an Agilent E4407B spectrum analyzer with a maximum operating frequency of 26.5 GHz as well. The detector itself was held at room temperature and mounted on a three-axis *xyz* stage for

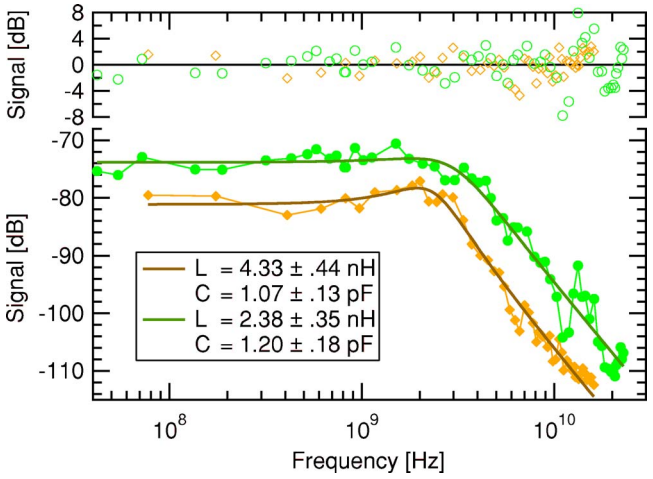

FIG. 4. (Color online) Frequency responses of a 5.35 μm QCD operated at room temperature and for two differently connected devices. The upper curve (circles) corresponds to a device with a 2.5 mm long bond wire, whereas the lower curve (squares) describes the mounting with the longer 4.5 mm bond. The dots are measured data points, whereas the two solid curves are fits using the *RLC* model mentioned in the text. The upper curves are errors between experiment and fit measured in decibels.

precise alignment. From the observed alignment sensitivity, we estimated that the spot size on the device was on the order of 250 μm in diameter. Figure 4 shows the measured and simulated frequency response before and after a careful rebonding with a slightly shorter bonding wire. When using the shorter wire, the cutoff frequency (3 dB point) was at roughly 4 GHz and the maximum modulation frequency observed was 23 GHz. At this maximal frequency, the signal was 35 dB lower than at 4 GHz. In the case of the longer wire, cutoff was at 3 GHz with a frequency maximum at 16 GHz. From the fitted (solid) lines in Fig. 4, it is obvious that in both cases, the cutoff behavior of the QCD can be simulated with the simple *RLC* circuit presented in Fig. 3(b). According to this model, in which we assume the detector to behave as a current source, the measured voltage as a function of frequency, $U_{\mathrm{meas}}(\omega)$, can be described by

$$U_{\mathrm{meas}}(\omega) = I \cdot |Z_\omega| = \frac{I \cdot R}{|1 + i\omega C \cdot (R + i\omega L)|},$$

where Z_ω is the total impedance of the circuit, R the 50 Ω input impedance of the first amplifier, C the parasitic capacitance of the QCD, L the parasitic inductance of the bond wire, and ω the angular frequency of the signal. Both parasitic inductance of the wire and capacitance of the QCD are used as fit parameters. On the other hand, we can also estimate these two quantities based on the physical dimensions. For a gold wire with a length $l=2.5$ mm, a radius $r=12.5$ μm, and $\mu_0=4\pi 10^{-7}$ H/m, as used in the 23 GHz experiment, we get an inductance $L=(1/2\pi)\ \mu_0\ l\ [\ln(2l/r)-1]=2.5$ nH, which is in good agreement with the fitted value of 2.4 nH. The same is true for a capacitance with an area $A=100\times 100$ μm^2, a thickness $d=1.65$ μm, and using InAlAs/InGaAs as a dielectric ($\varepsilon=15$, $\varepsilon_0=8.85\times 10^{-12}$ A s/V m, all dimensions correspond to the actual device). In this case, we get $C=\varepsilon_0\varepsilon(A/d)=0.82$ pF which agrees reasonably well to the fitted value (1.08 pF). It is thus clear that the cutoff of the QCD signal is not due to the internal mechanism of the device but rather due to its size and type of connection. An estimation of the transport time from the excited state to the ground state by subsequent electron-phonon scattering yields a value on the order of 5–10 ps. Together with an intersubband absorption time of 2.5 ps and a tunneling time of 0.15 ps (computed via the Kazarinov-Suris model),[14] we can conservatively deduct a total transport time $\tau=15$ ps. Assuming further that the 3 dB frequency is computed via $\omega_{3\ \mathrm{dB}}=1/\tau$, we end up with a cutoff frequency of roughly 65 GHz. For future experiments, we expect that a careful impedance matching using a microstrip line and a circular mesa with 50 μm diameter will result in a cutoff frequency which lies closer at this theoretical limit.

In summary, we have designed, fabricated, and tested an InGaAs/InAlAs-based QCD for 5.35 μm. Such devices are operated without external bias voltage and therefore do not suffer from dark current noise. Due to their narrow spectral sensitivity curve, they are very selective; this again has a positive effect on the noise properties. Finally, their excellent high frequency behavior—up to 23 GHz modulation frequency—and their responsivity at room temperature are very promising for applications in astronomical heterodyne interferometry, but also for terrestrial staring applications in focal plane arrays or for characterization of ultrashort mid-infrared laser pulses.

The authors gratefully acknowledge the Professorship program of the Swiss National Science Foundation for financial support; Alexis Bögli from the Electronics Group at the Institute of Microtechnology, University of Neuchatel, and Hansruedi Benedickter from the Microwave Electronics Group at ETH, Zurich for technical assistance; and Nicolas Hoyler and Marcella Giovannini (both from Institute of Physics, University of Neuchatel) for growing the material.

[1] D. Hofstetter, M. Beck, and J. Faist, Appl. Phys. Lett. **81**, 2683 (2002).
[2] L. Gendron, M. Carras, A. Huynh, V. Ortiz, C. Koeniguer, and V. Berger, Appl. Phys. Lett. **85**, 2824 (2004).
[3] M. Graf, N. Hoyler, M. Giovannini, J. Faist, and D. Hofstetter, Appl. Phys. Lett. **88**, 241118 (2006).
[4] C. Schönbein, H. Schneider, G. Bihlmann, K. Schwarz, and P. Koidl, Appl. Phys. Lett. **68**, 973 (1996).
[5] M. Graf, G. Scalari, D. Hofstetter, J. Faist, H. Beere, G. Davies, E. Linfield, and D. Ritchie, Appl. Phys. Lett. **84**, 475 (2004).
[6] S. Ehret, H. Schneider, J. Fleissner, P. Koidl, and G. Böhm, Appl. Phys. Lett. **71**, 641 (1997).
[7] D. D. S. Hale, M. Bester, W. C. Danchi, W. Fitelson, S. Hoss, E. A. Lipman, J. D. Monnier, P. G. Tuthill, and C. H. Townes, Astrophys. J. **537**, 998 (2000).
[8] K. A. Briggman, L. J. Richter, and J. C. Stephenson, Opt. Lett. **26**, 238 (2001).
[9] E. D. Hinkley, T. C. Harman, and C. Freed, Appl. Phys. Lett. **13**, 49 (1969).
[10] P. D. Grant, R. Dudek, L. Wolfson, M. Buchanan, and H. C. Liu, Electron. Lett. **41**, 69 (2005).
[11] H. C. Liu, J. M. Brown, K. Z. McIntosh, K. B. Nichols, and M. J. Manfra, Appl. Phys. Lett. **67**, 1594 (1995).
[12] D. Hofstetter, M. Beck, T. Aellen, and J. Faist, Appl. Phys. Lett. **78**, 396 (2001).
[13] H. C. Liu, M. Buchanan, and Z. R. Wasilewski, Appl. Phys. Lett. **72**, 1682 (1998).
[14] R. F. Kazarinov and R. A. Suris, Sov. Phys. Semicond. **5**, 707 (1971).